



ESTIMATION OF SEDIMENT THICKNESS BY USING MICROTREMOR OBSERVATIONS AT PALU CITY, INDONESIA

By

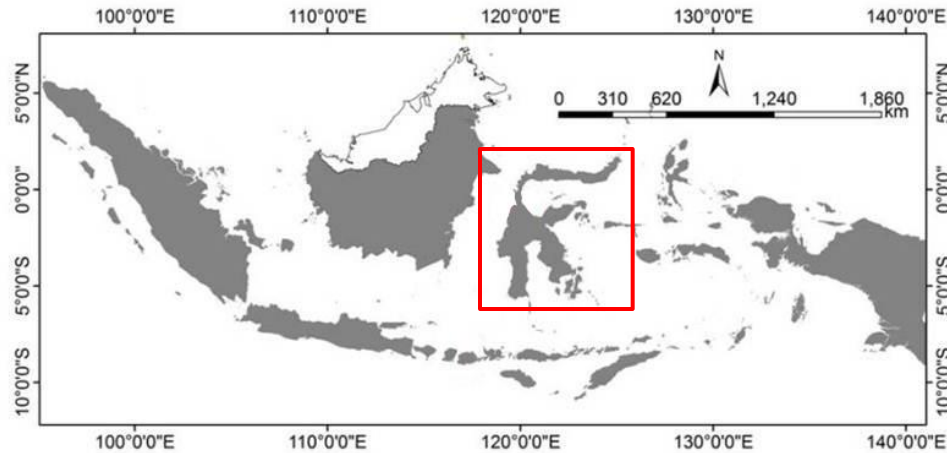
Pyi Soe Thein

11 November 2013

Outlines

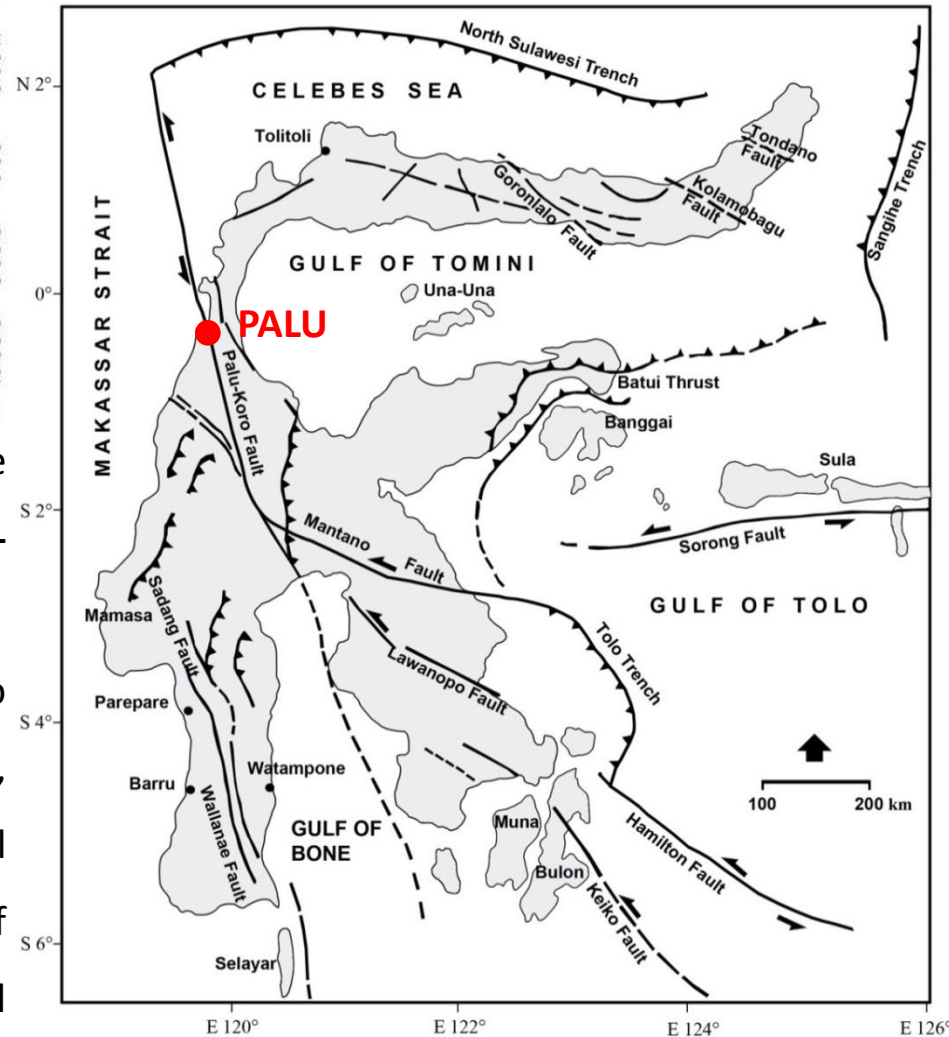
- **Introduction**
- **Research objectives**
- **Research analyses**
- **Microtremor Single station
observaions**
- **Microtremor Array observations**
- **Discussion**

Introduction



➤ Located in the triple junction of collision between the major plates: **Eurasia**, **Eastern Pacific** and **Indo-Australia**.

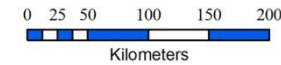
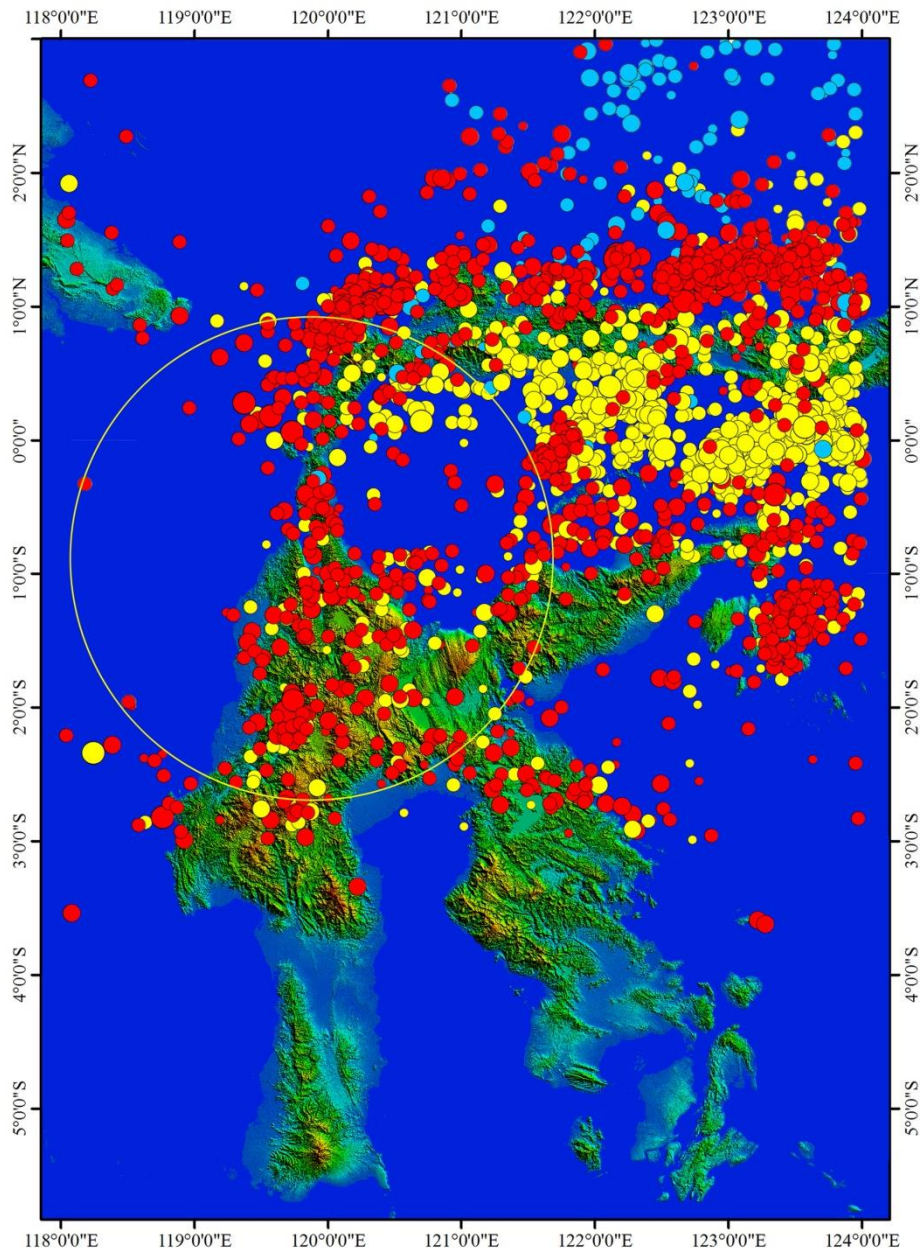
➤ Evolution of Neogene kinematics along the Palu-Koro fault was confirmed based on microtectonics approach, i.e.: **sinistral strike-slip** due to **E-W compression**, radial extensions caused by telescoping vertical movement of **Neogene granitoid**, and then left lateral with normal component displacement due to **N-S extension/ E-W compression** which is still active actually (Pamumijoyo et al., 1997).



**Tectonic Map of Sulawesi
(Compiled by Priadi , 1993)**

Introduction

Seismicity



Source : BMKG, ISC & USGS website

LEGEND

Magnitude

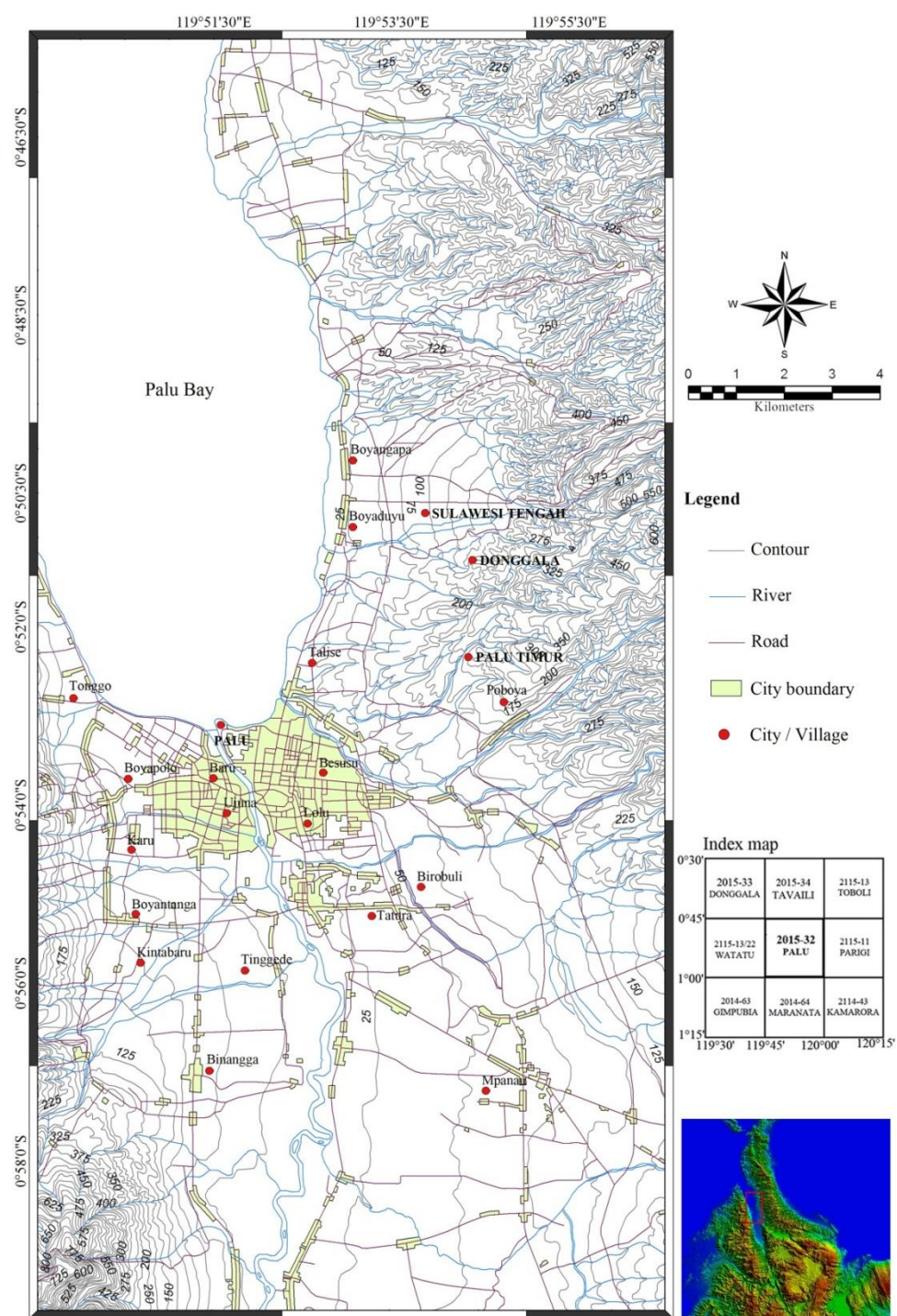
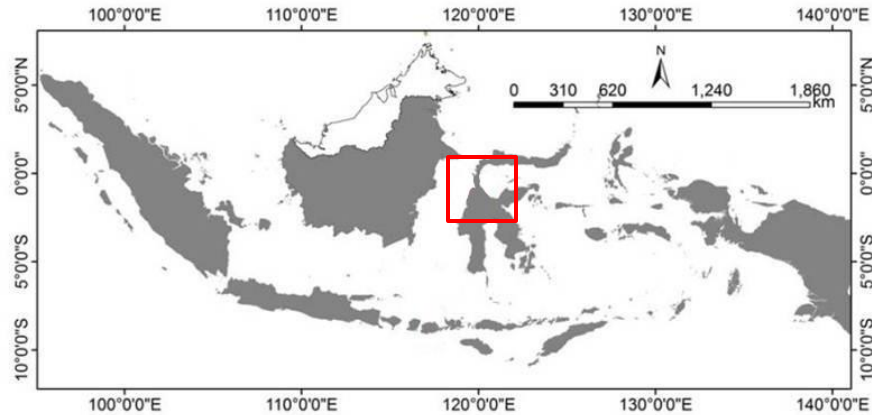
- 3.0 - 3.9
- 4.0 - 4.9
- 5.0 - 5.9
- 6.0 - 6.9
- ≥ 7.0

Depth (Km)

- < 70
- 70 - 300
- > 300

Epicentral distribution of some important earthquakes around Palu province (1968-2012). (Geological Engineering Department Gadjah Mada University, 2012)

Introduction



**Location of the study area,
Palu City, Central Sulawesi,
Indonesia**

Introduction



**Panoramic View of Palu City from West escarpment,
Central Sulawesi, Indonesia**

Research Objectives

To provide sediment thickness or the depth of subsurface engineering bed rock from microtremor array observation

To analyze amplification characteristics for Palu area by using trench data, borehole data and microtremor method

To calculate the strong ground motion for some selected previous earthquakes compared with their damage distribution

To provide a comprehensive summary of the main methods and techniques used in seismic microzoning

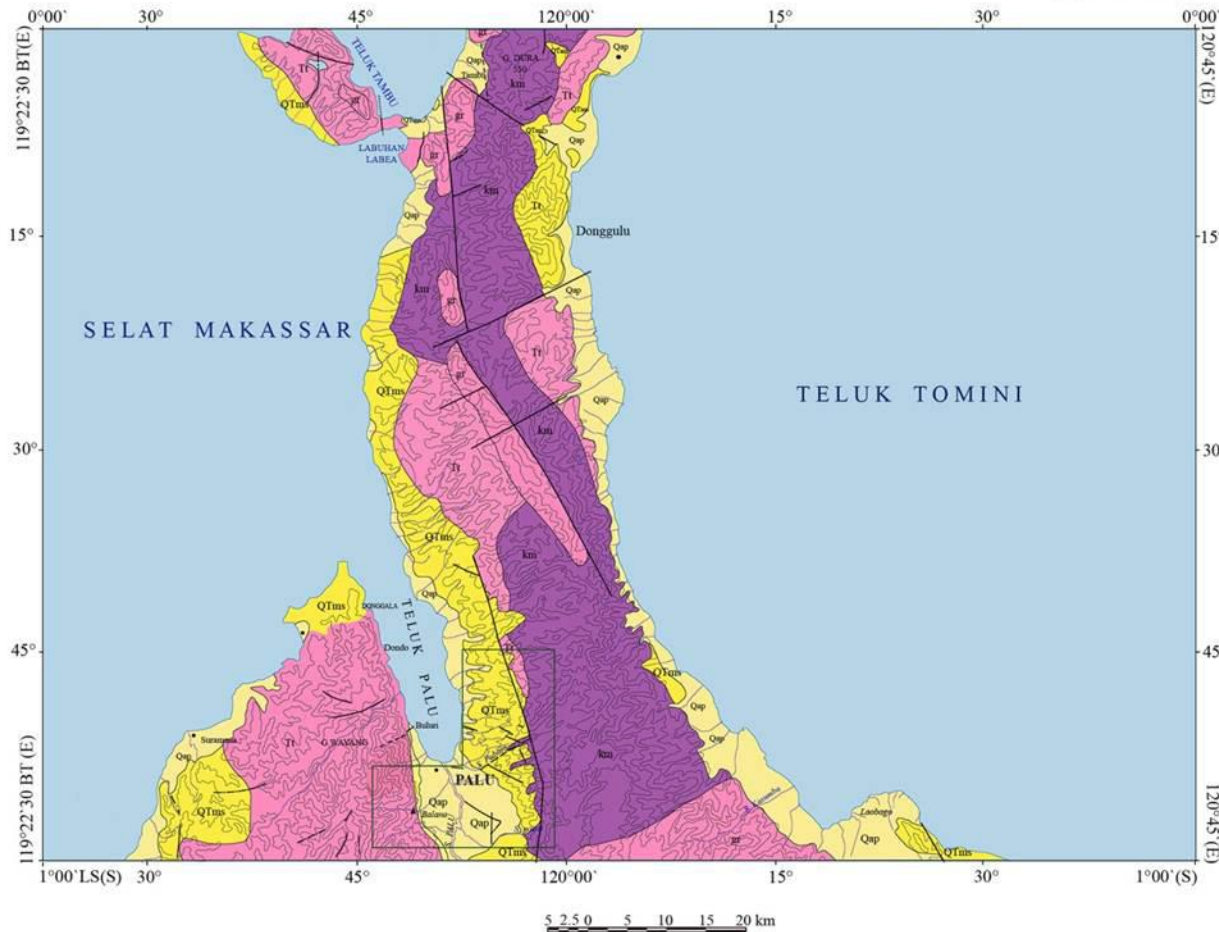
Research Analyses

**Microtremor single station
observations**

Microtremor Array Observations

Geology of Palu Area

PALU-2015 & 2115



EXPLANATION

- Qap** Alluvium and coastal deposits
gravel, sand, mud and coral limestone
- QTms** Celebes Molasse of Sarasin (1901)
Conglomerate, sandstone, mudstone, coral limestone, and marl, in part weakly consolidated (where dominantly limestone)
- Tt** Tinombo Formation of Ahlburg (1913), as used by Brouwer (1934)
Shale, sandstone, conglomerate, volcanic rocks, limestone and chert; includes phyllite, slate and quartzite near intrusion (where dominantly volcanic rocks)
- km** Metamorphic complex
Mica schist, amphibolitic schist, gnesis, and marble (where dominantly gnesis)
- gr** Granite and granodiorite



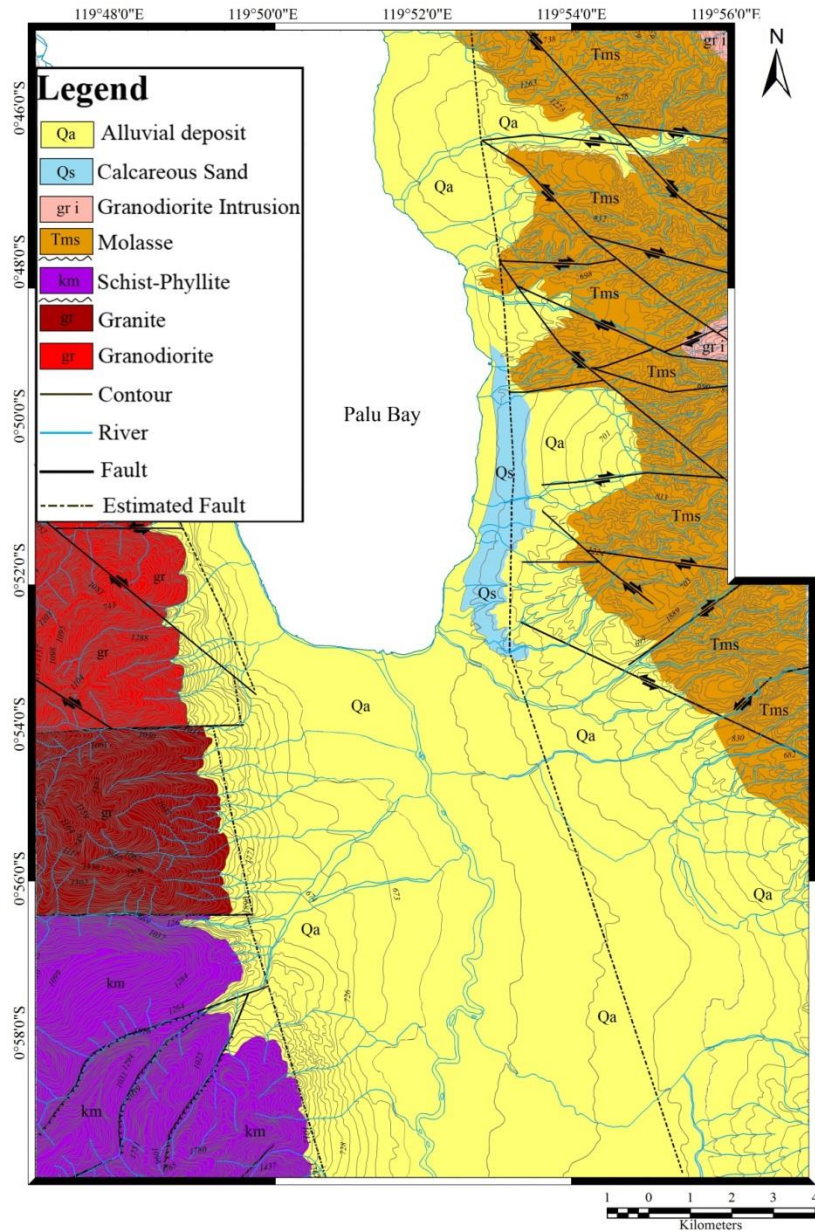
STUDY AREA

RECONNAISSANCE GEOLOGICAL MAP OF THE PALU QUADRANGLE, SULAWESI

BY
RAB SUKAMTO

H.SUMADIRDJA. T. SUPTANDAR.S. HARDJOPRAWIRO dan (and) D.SUDANA
1973

Geology of Palu Area



Geological Map of Palu Depression Area
(Indra, Imawan, Pohan and Juwanto, 2012)

Alluvium and Coastal Deposits



- A. Fossiliferous limestone in Alluvium deposits. (S $00^{\circ}49.29.3'$ and E $119^{\circ}53.08.1'$)
- B. Coastal Deposits with some fossil fragment in vertical position. (S $00^{\circ}49.29.3'$ and E $119^{\circ} 53.08.1'$)

Celebes Molasse of Sarasin (1901)



A. Celebes Molasse consists of mudstone. (S $00^{\circ}52.204'$ and E $119^{\circ}53.317'$)

B. Alteration of sandrock and massive clay in Celebes Molasse. (S $00^{\circ}52.2293'$ and E $119^{\circ}53.317'$)

Metamorphic Complex



- A. Typical features of schist exposed on western ridge of Palu area. (0814790 and 98894972)
- B. B. Folded schist exposed only on western ridge of Palu area. (081298 and 9890521)

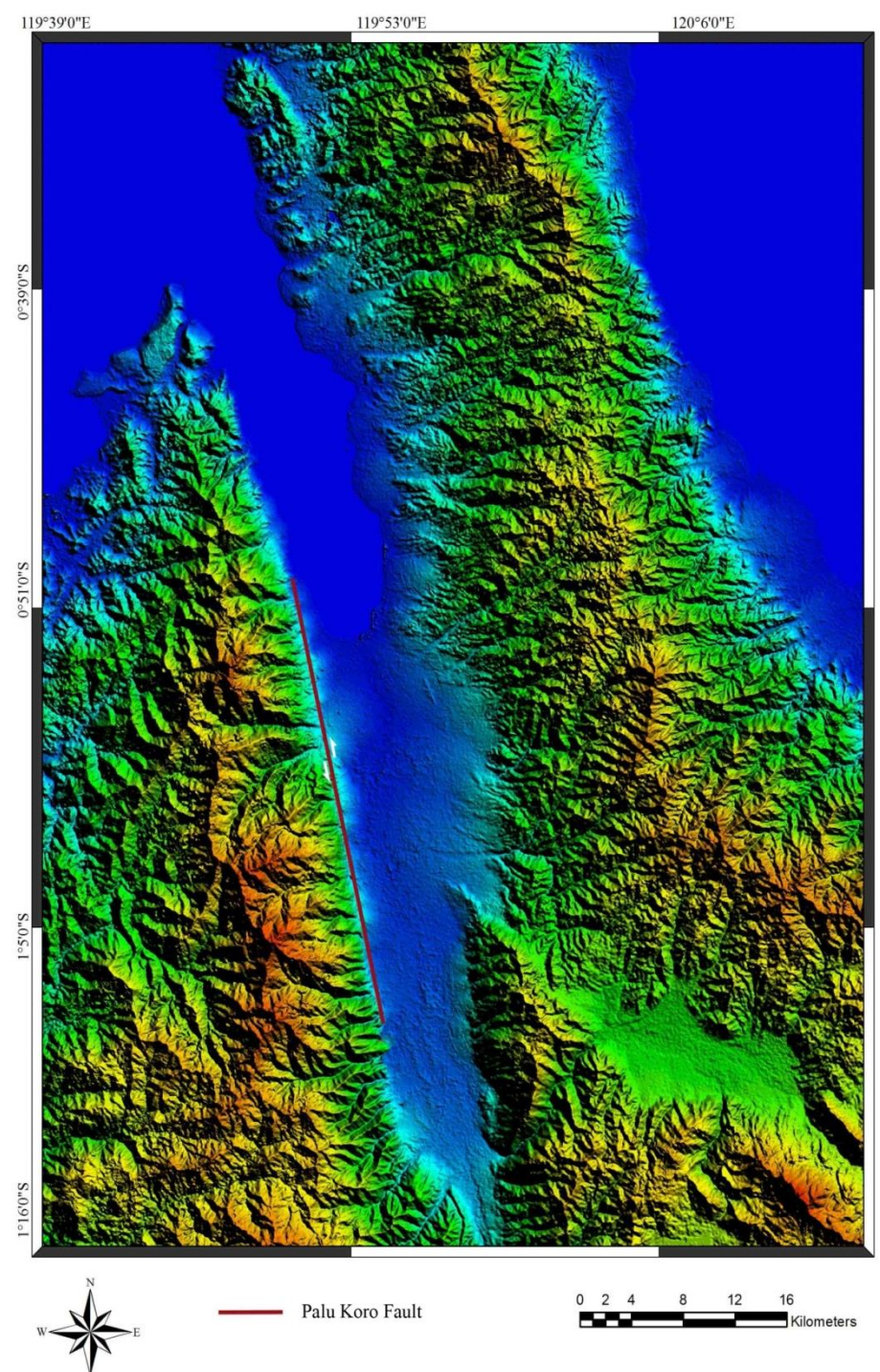
Intrusive Rocks



- A. Igneous rock intruded in northwestern part of Palu area. (S 00°49.184' and E 119°47.526')
- B. Granite intruded in western part of Palu area. (S 00°51.992' and E 119°49.142')

Palu-Koro Fault

ASTER GDEM landsat image showing some structural features of the Palu-Koro Fault system.



Microtremor

➤ Microtremor(s)

- Constant vibrations of the Earth's surface
- The surface of the Earth is always in motion without earthquake.

➤ Very small amplitude

- Displacement : $10^{-4} - 10^{-2}$ mm
- Far from human sensing

Single Station Observations

- A three-component accelerometer with data logger, GPL-6A3P, produced by the Mitsutoyo Co. Ltd., was used.
- The number of single point observations was **151** sites
- The sampling frequencies were **100 Hz or 500 Hz** and the observation times were **10 to 15** minutes.
- Using 3 Component (Two Horizontal and One Vertical) Sensor
- **DATA ANALYSIS: Horizontal to Vertical Spectrum Ratio (HVSr) Method**



Instrument of GPL 6A-3P
(Mitsutoyo), Akashi Co. Ltd.



Instrument of Network Sensor
Model VC-374 AVT.

Single Station Observation

HVSR Method (Nakamura Method)

3 Component Sensor



H/V Spectrum Ratio:

$$H/V(\omega) = \frac{\sqrt{(F_{NS}(\omega))^2 + (F_{EW}(\omega))^2}}{F_{UD}(\omega)}$$

Recorded
microtremor

NS 

EW 

UD 

FFT



$F_{NS}(\omega)$

FFT



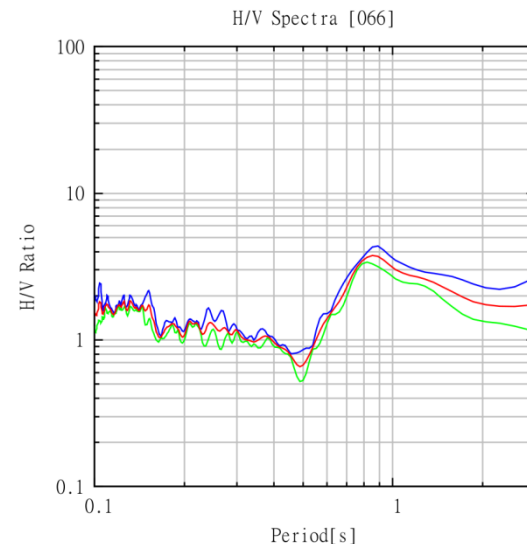
$F_{EW}(\omega)$

FFT

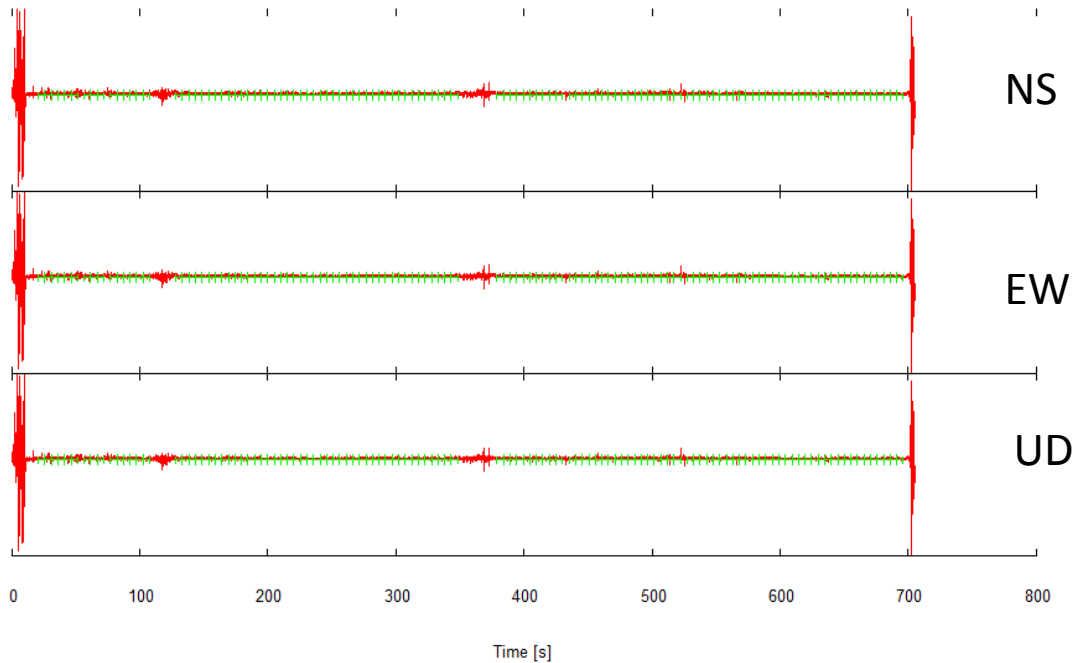


$F_{UD}(\omega)$

Peak Period -> Site Dominant Period



BIDO Software

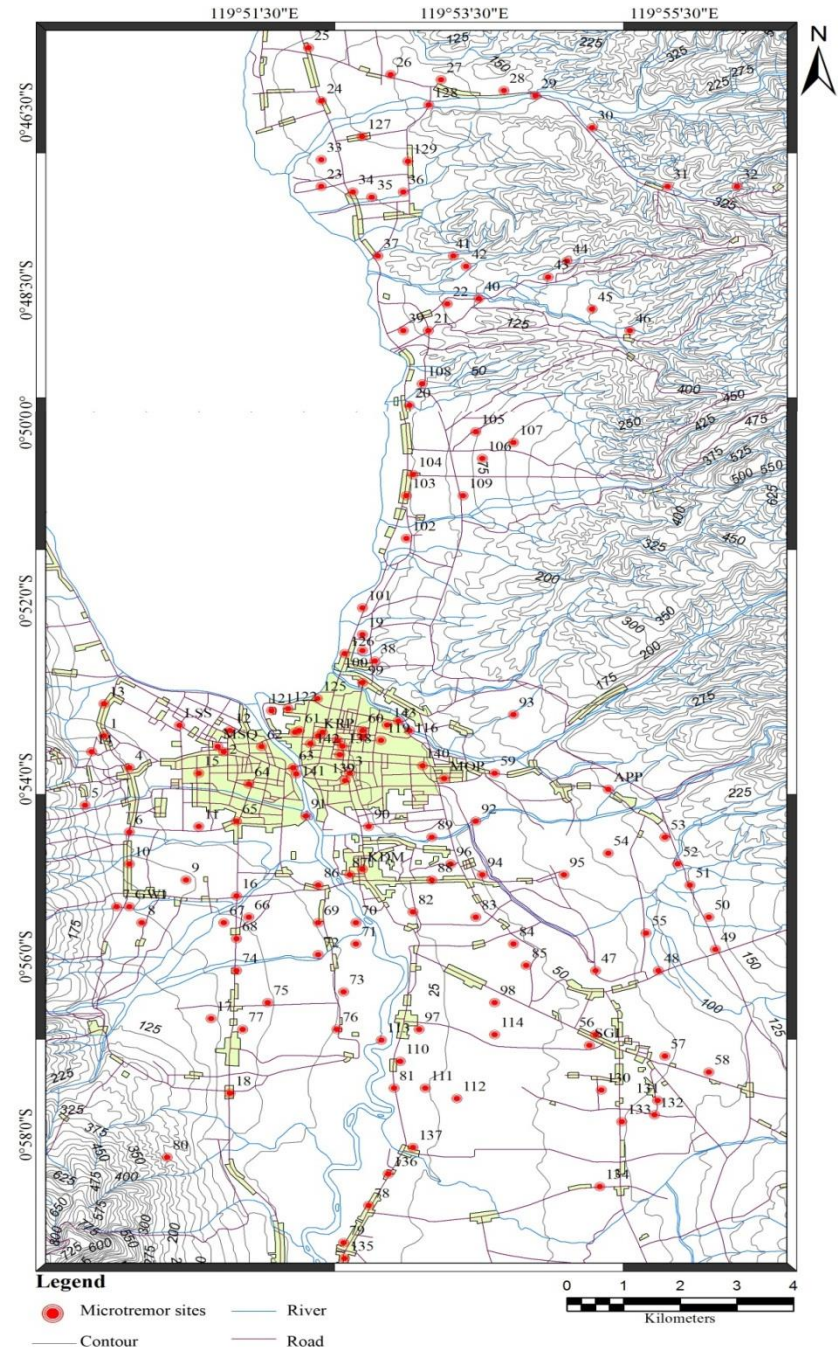


- Duration of data segments for the evaluation of spectra [s] is 10.24
- Spectral window [Hz] is 0.3

Single Station Observations



151 single station Microtremor observation sites at Palu city area

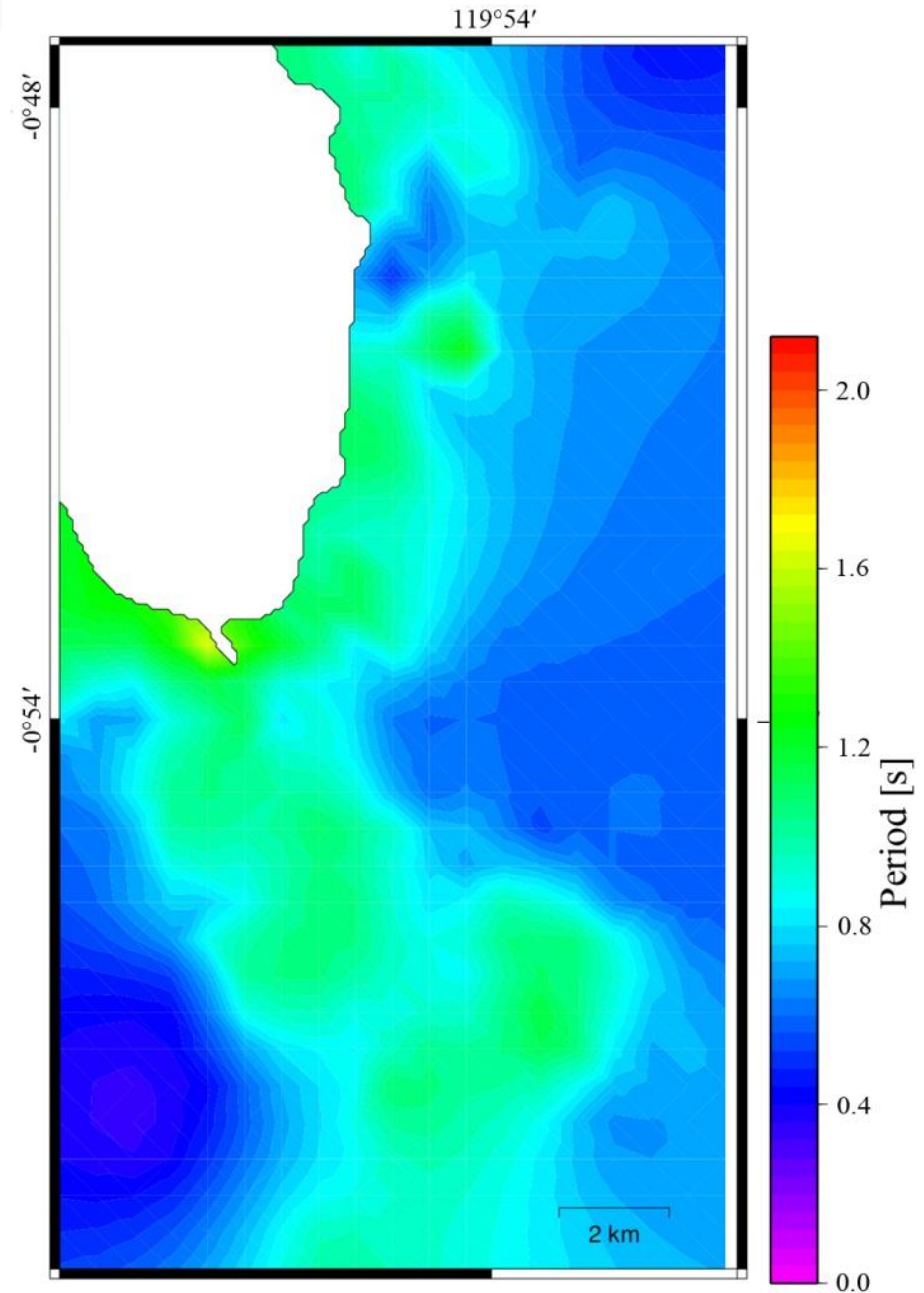
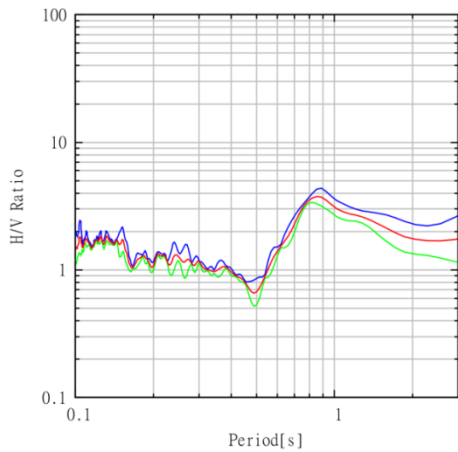
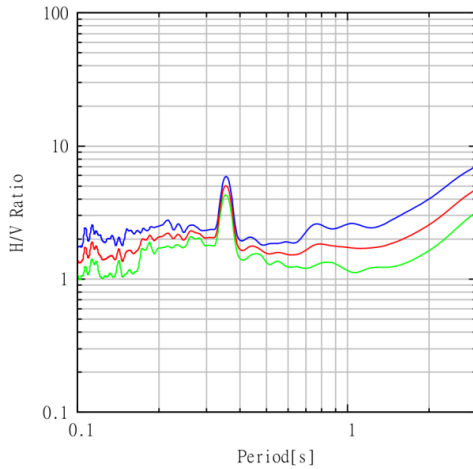


Predominant Period[s]

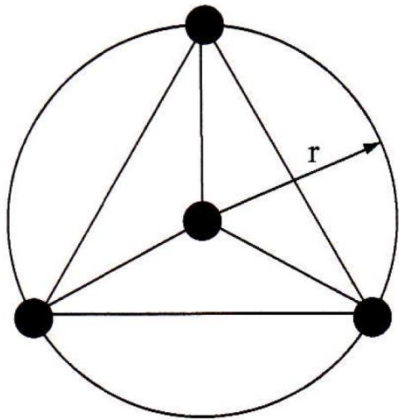
- Space interpolation is conducted by ordinary kriging technique
- The predominant periods of 1.0-1.8 seconds were on the alluvial fan area.
- The spatial correlations between predominant periods on the west side mountain, of which slope is steep, are shorter than those in the east side mountain and change more rapidly

Predominant Period[s] Map

- Type A: with short period peak
- Type B: with long period peak
- Type C: those without clear peaks



Array Observations

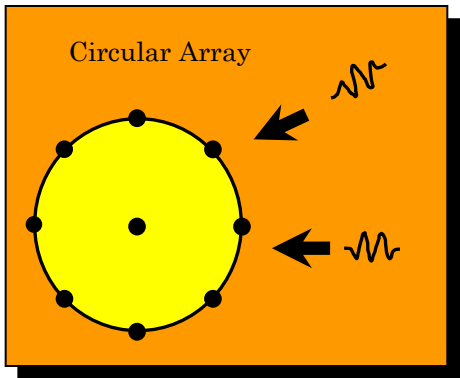


Triangle Array

Array geometry (Black circles: sensors)		
Total number of sensors		4
At the center		1
Around the circle		3
Vertical motion alone	Phase velocities of Rayleigh waves	SPAC CCA nc-CCA H0, H1, V
	Phase velocities of Love waves	None

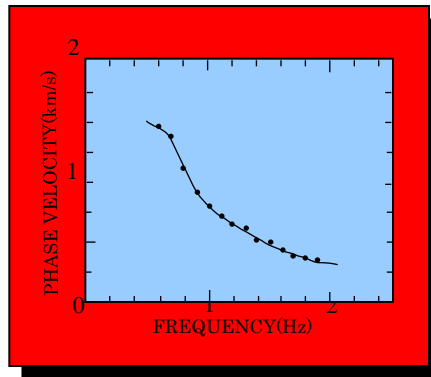
Array Observations

Microtremor Observation

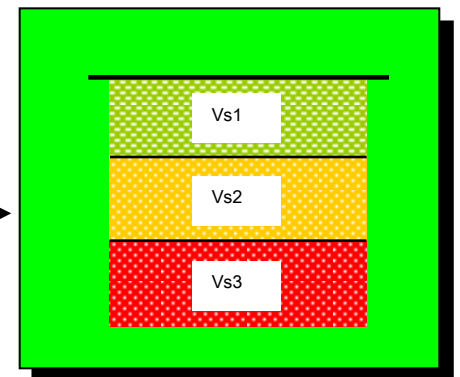


SPAC
Method

Dispersion Curve

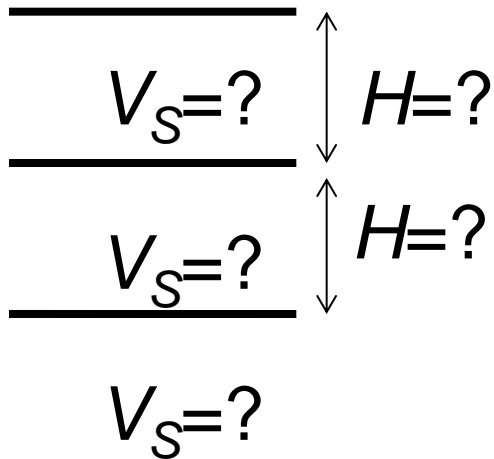


Shear Wave Velocity Profile



Constructing subsurface profile by inversion analysis

Assume shear wave profile



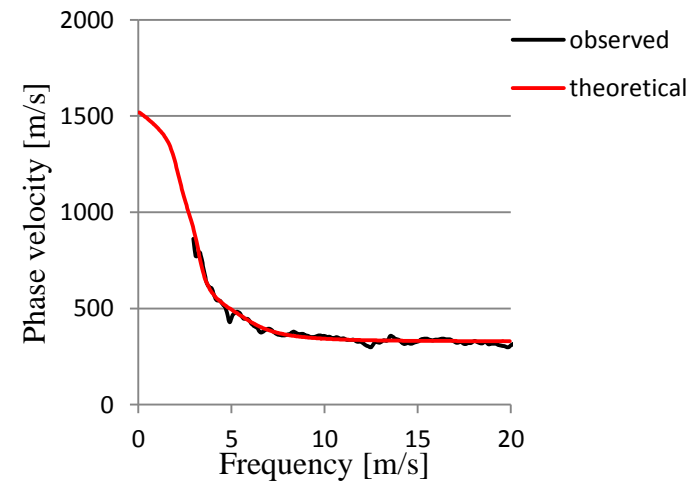
Calculating Dispersion Curve
(Theoretical)



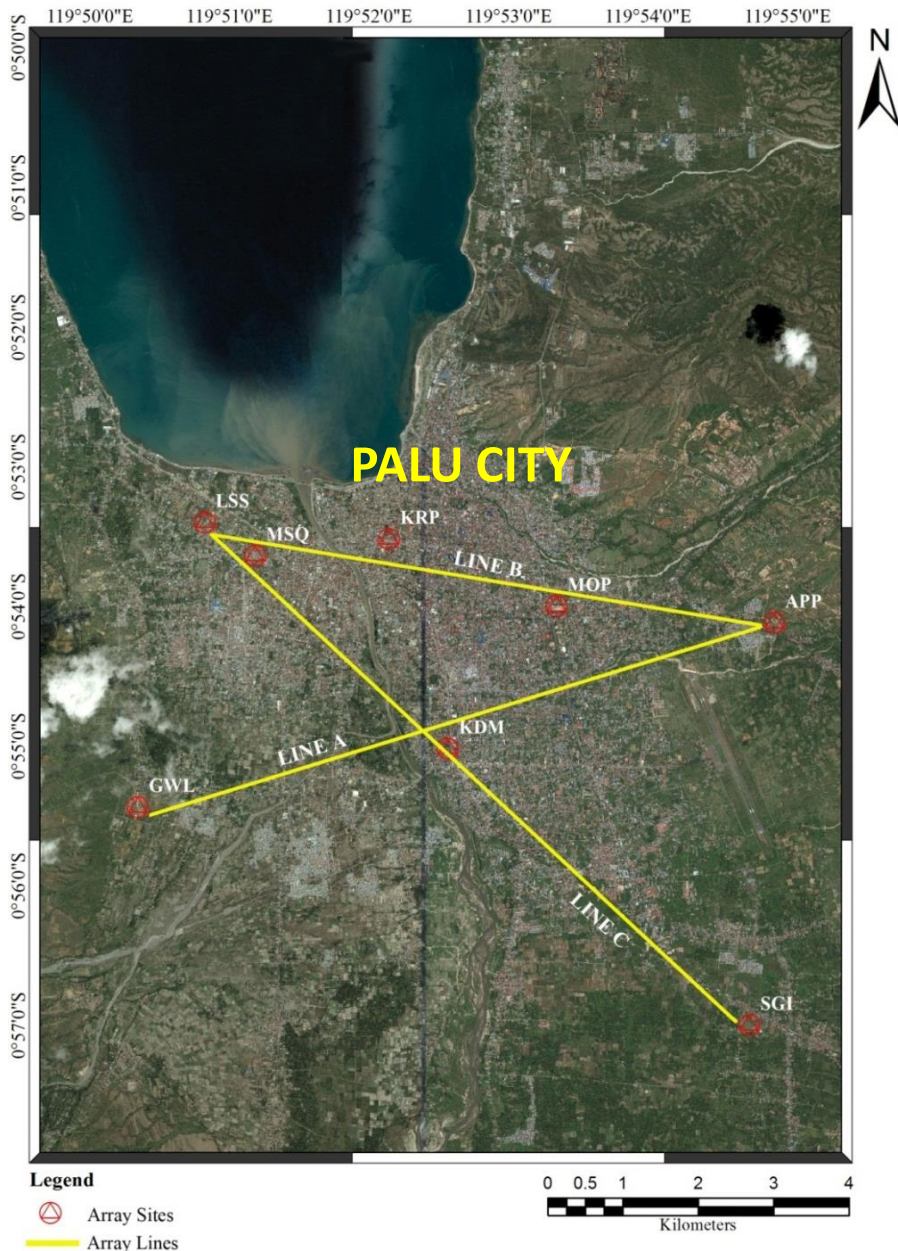
Compare theoretical D.C. with
Observed one



Update Profile



Array Observations

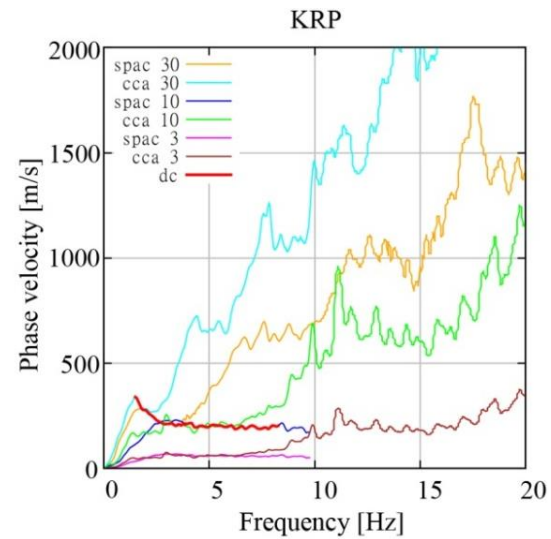
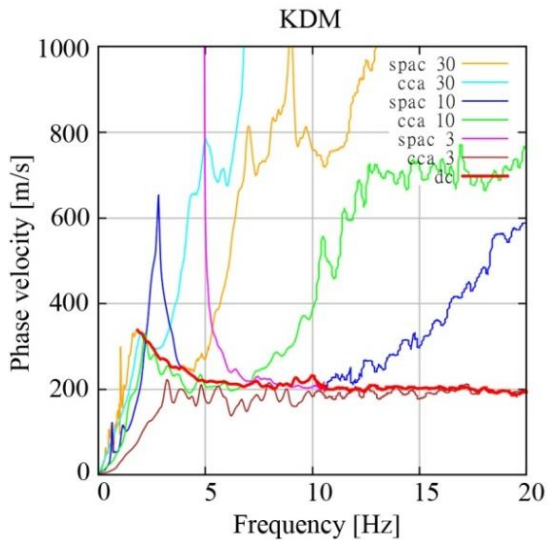
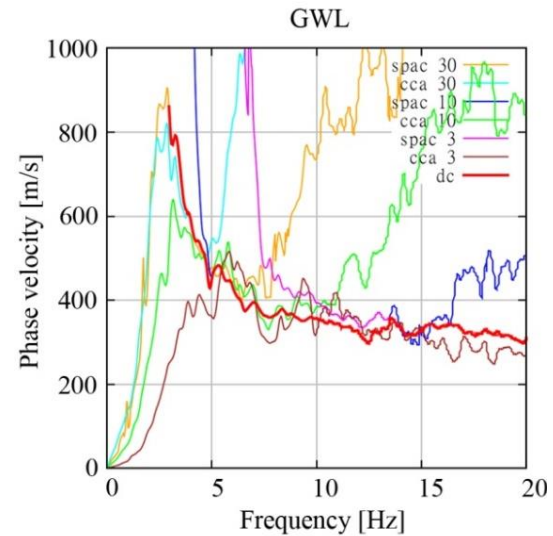
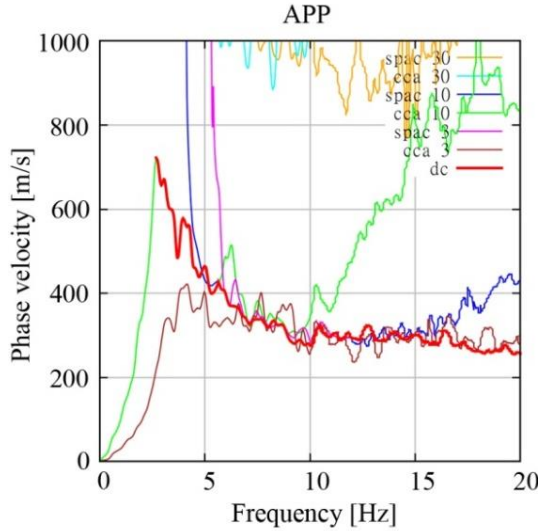


- The number of array observations was **8** sites.
- The sampling frequencies were 1000 **Hz** and the observation times were **10 to 30 minutes**.
- Radius **3 meter, 10 meter and 30 meter** at each array sites.

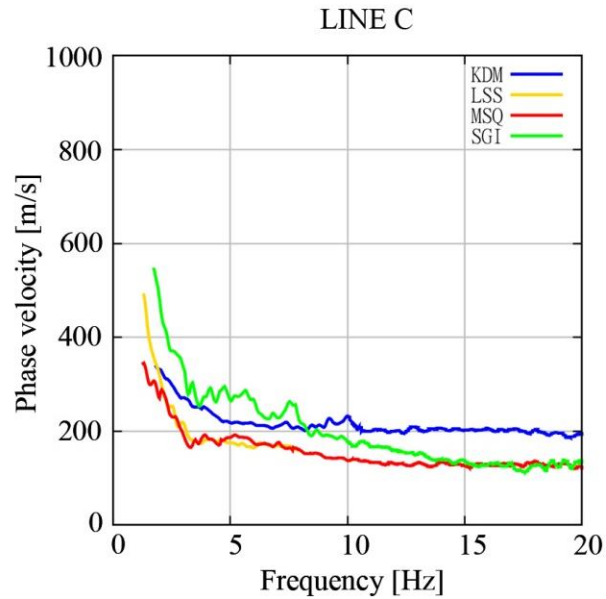
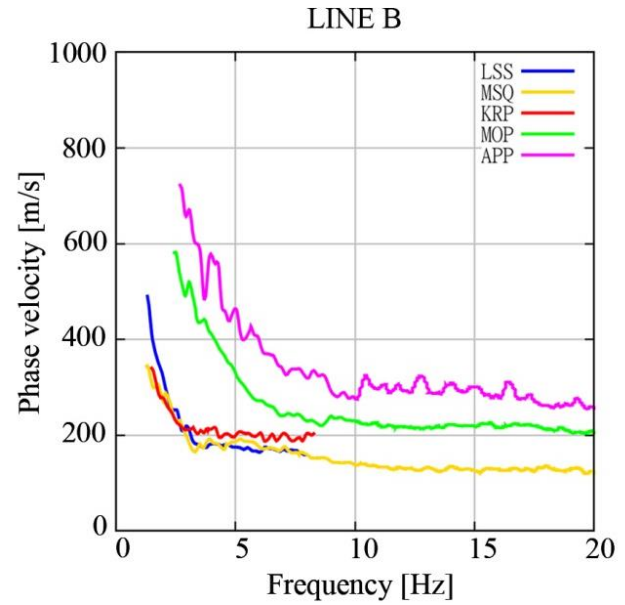
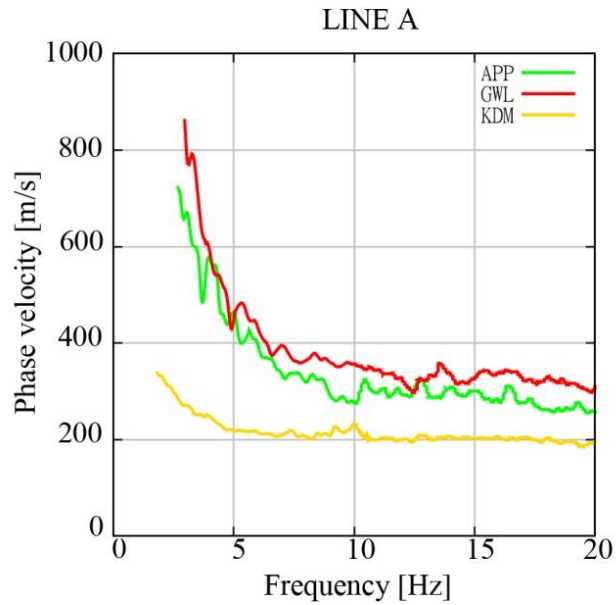
Phase Velocity by Dispersion Curves

- A spatial autocorrelation coefficient for a **circular array** can then be defined when the waves composing the microtremor (i.e., the subsurface waves) are dispersive.
- The **spatial autocorrelation** is a function of **phase velocity and frequency**.
- Rayleigh wave records were measured for **the 8 array observation sites** using the SPAC method and inversion analysis was undertaken on the observed dispersion curves to estimate the **soil profiles**.
- In the inversion analysis, the **Particle Swarm Optimization (PSO)** algorithm was adopted to solve the non-linear optimization problem

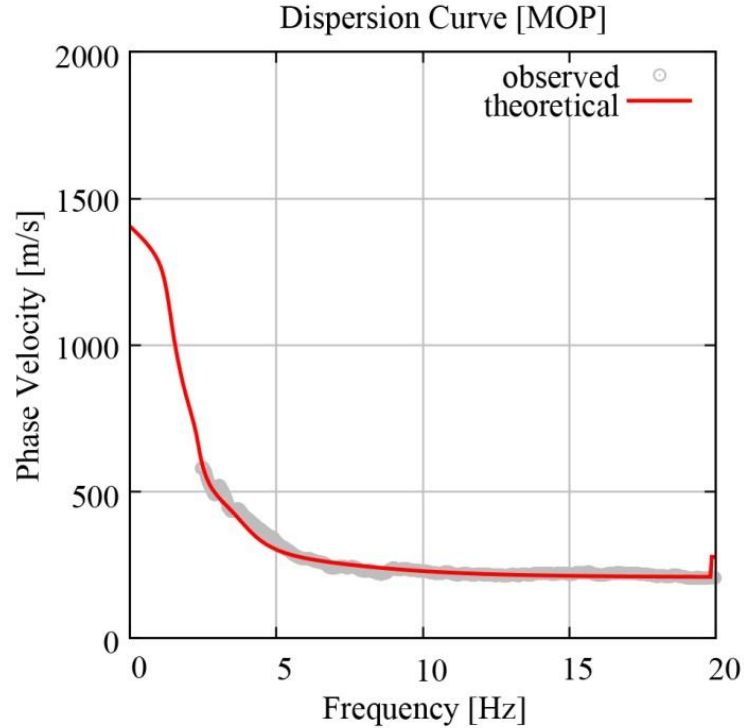
Phase Velocity by Dispersion Curves



Three Survey Lines



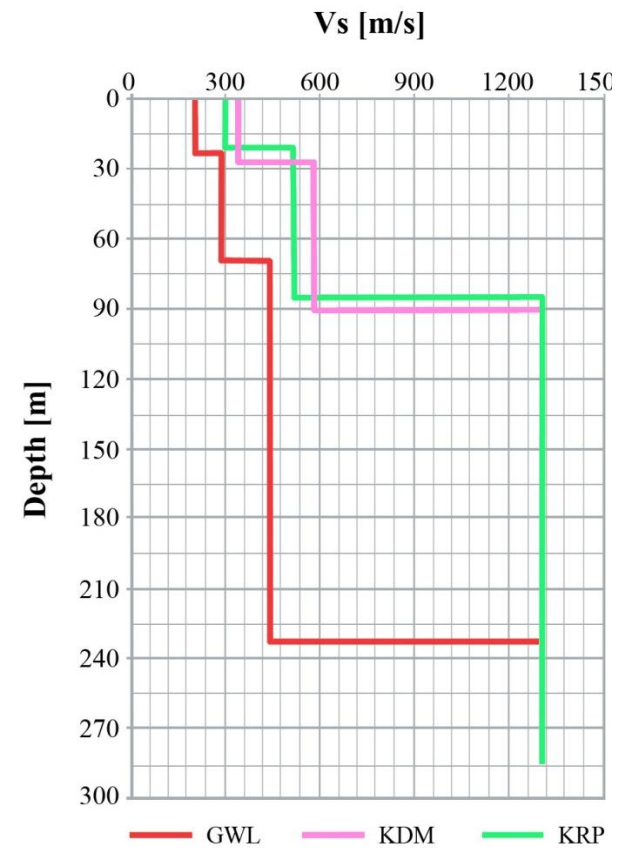
Estimated Ground Structure



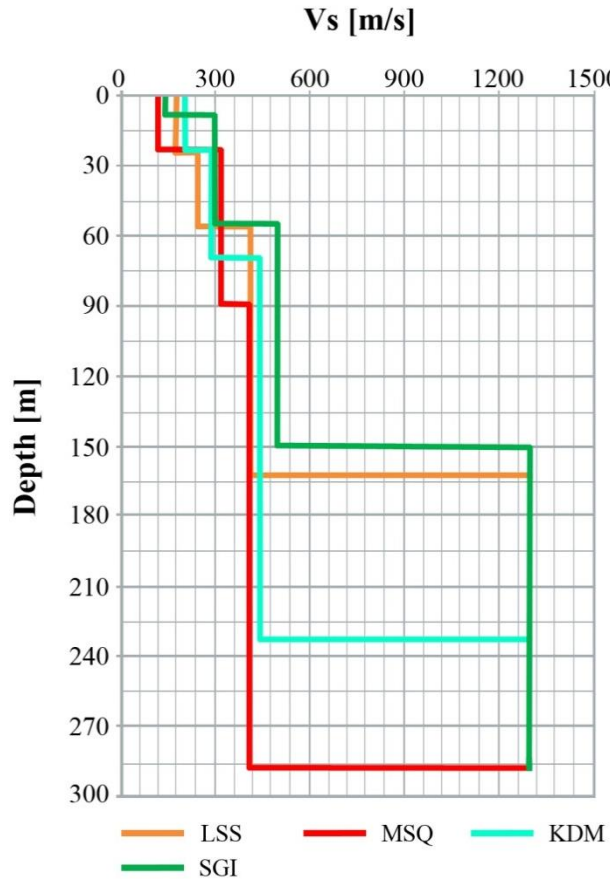
Layer No.	ρ [t/m ³]	Vp[m/s]	Vs[m/s]	H[m]
1	1.7	1066.9	218.1	11.1
2	1.8	1245.2	292.9	21.9
3	1.9	1717.0	532.9	84.0
4	2.4	3125.8	1502.5	Infinity

MOP (Mayor of Palu)

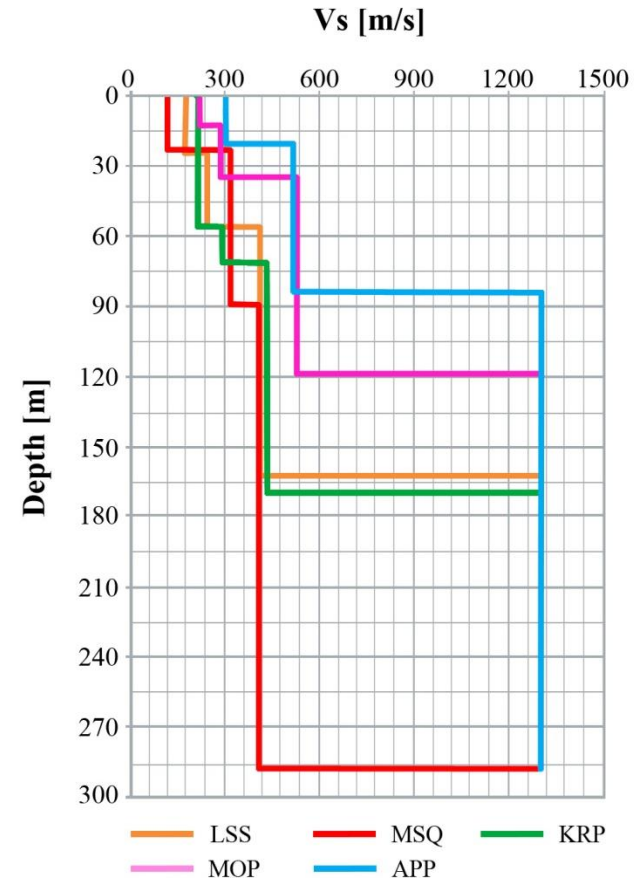
Vs Structure along the Survey Lines



↑
LINE A

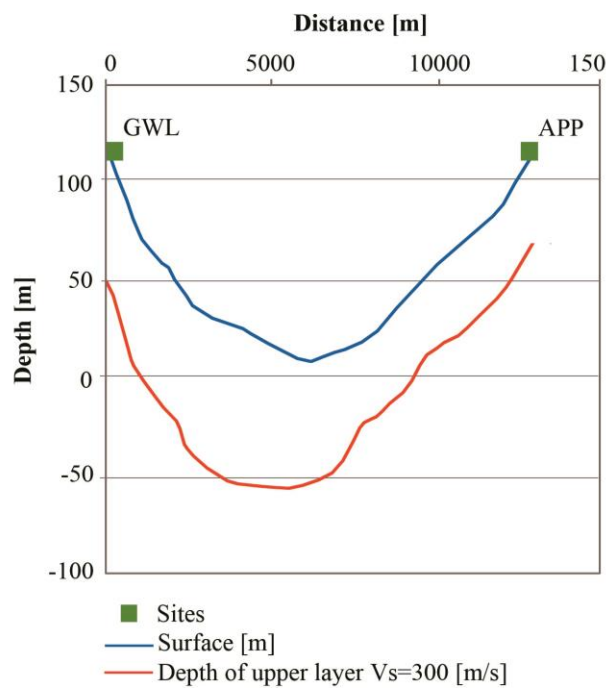


↑
LINE B

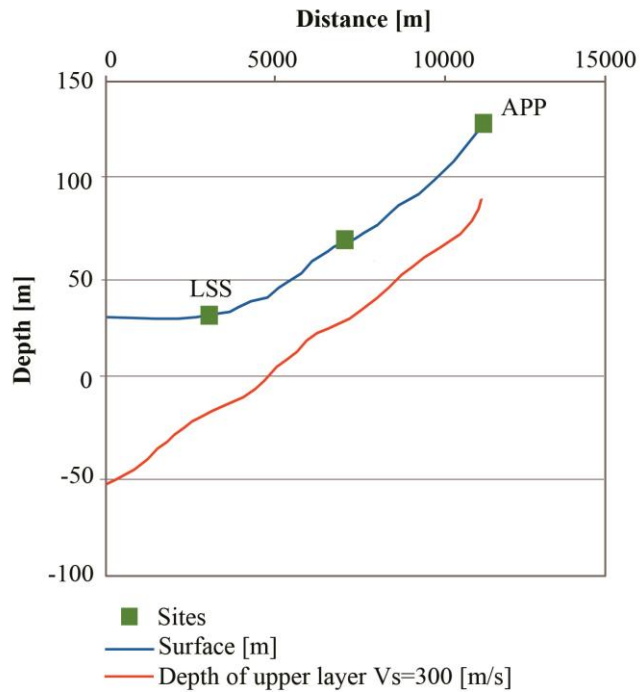


↑
LINE C

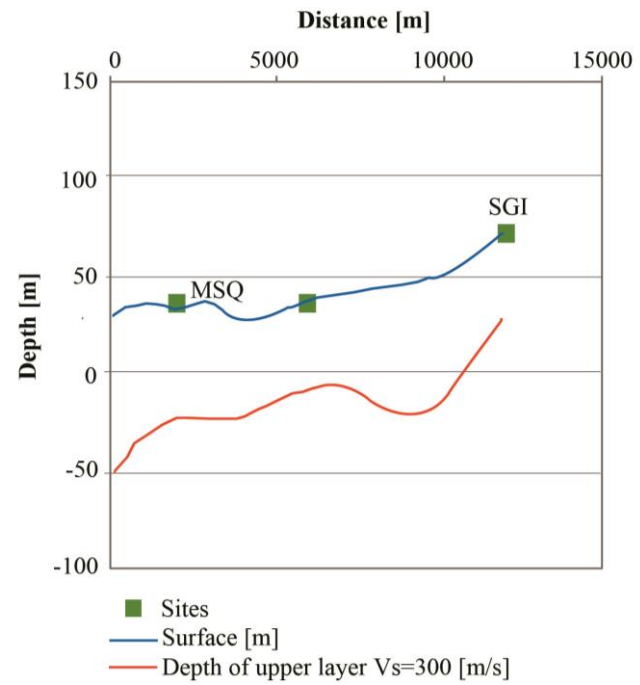
Two Dimensional Model



↑
LINE A



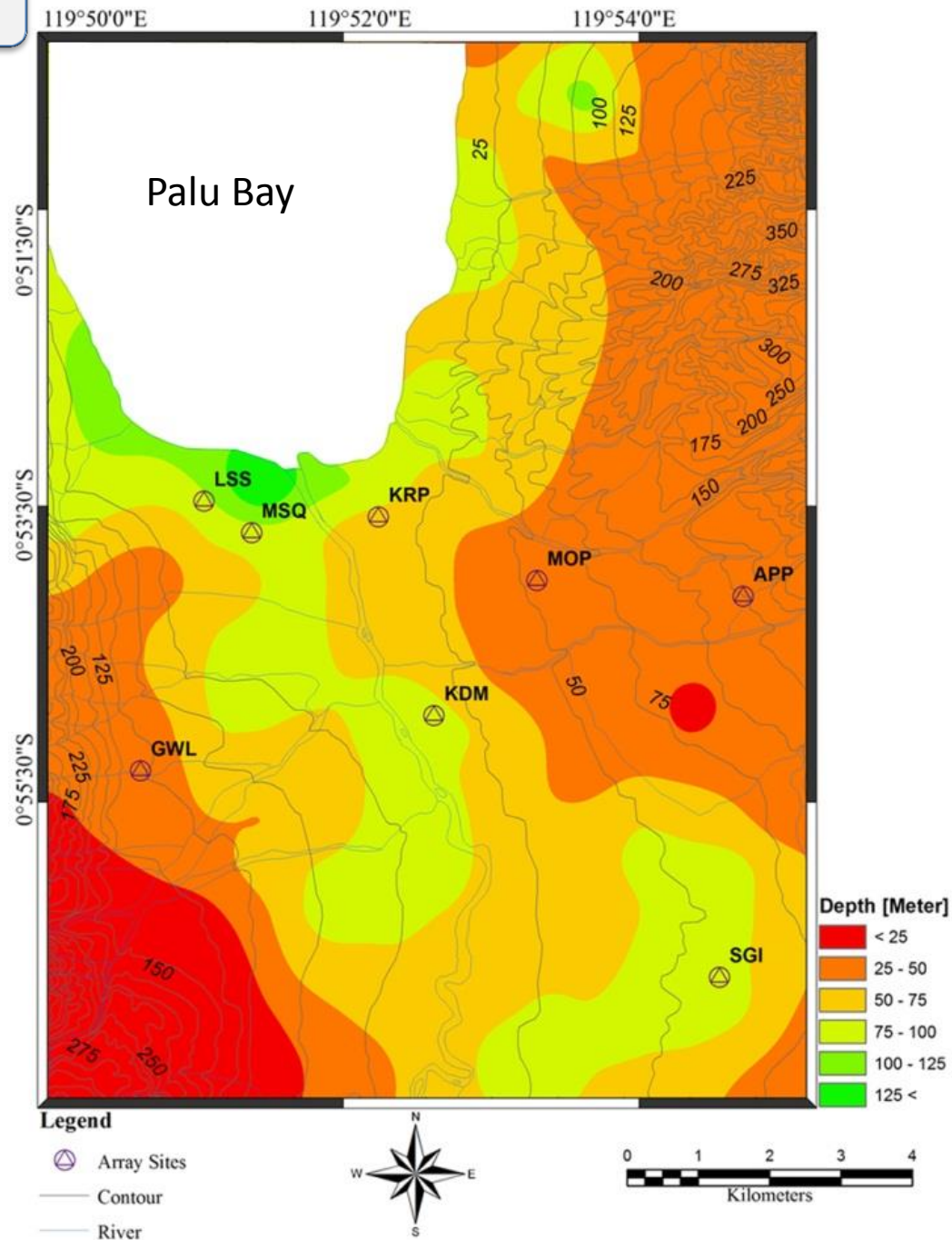
↑
LINE B



↑
LINE C

Sediment Thickness Map

$$H' = \frac{1}{4} \cdot \overline{V_s} \cdot T$$



Discussion

- Dominant in loose to medium dense **sand, silt and clay** sediments.
- Used by **Kriging method** (the interpolation of subsurface information such as predominant period, shear wave velocity and depth of irregular boundary)
- Possess **hard layers in upper most 125 m and weaker sediments underlain up to 25 m depth.** (According to the S-wave velocity structures from **array observation**)

**Thank you very much
for your kind attention**

Concluding and Remarks

- Microtremor observations were carried out for constructing a **subsurface ground model** in Palu.
- **Single-point** observations and **array** observations were conducted at **151** and **8** sites respectively, which covered almost the whole city area.
- H/V spectra were calculated at all the single observation sites and a distribution of **predominant periods** was obtained.
- The dispersion curves of a Rayleigh wave were obtained from the data of **array observations**.
- **The Kriging method** can be used for the interpolation of subsurface information such as predominant period, shear wave velocity and depth of irregular boundary.
- By conducting an inversion analysis for the calculation of **dispersion curves**, the **subsurface structure** beneath the site can be estimated.
- Constructed a **three layered model** in each array observation point.

Concluding and Remarks

- This research was reconstructed unified two-layered model by averaging the first three layers obtained from array observation. The shear wave velocity of the **top layer** is **V_s 300 m/s**. Three dimensional structure for shear wave velocities were **(I) $V_s \leq 300$ m.s, (II) $300 < V_s < 1300$ m/s and (III) $V_s > 300$ m/s**.
- By combining above two-layer model and the results of single point observation, the distribution of the first layer **thickness of the sediment is obtained**.
- The shear wave velocity structure and map of $V_s 300$ of studied area had been successfully determined together with **three dimensional model** of sediment thickness or depth of engineering bedrock.
- It is well observed that **S-wave velocity structure** play an essential role in response analysis and determination of sediment thickness or depth of engineering bedrock.
- The shear wave velocity structure and map of $V_s 300$ of studied area had been successfully determined together with **three dimensional model of sediment thickness or depth of engineering bedrock**.
- It is well observed that S-wave velocity structure play an essential role in response analysis and determination of sediment thickness or **depth of engineering bedrock**.